

Magnetic-field-induced shift of the optical band gap in $\text{Ni}_3\text{V}_2\text{O}_8$ P. Chen,¹ B. S. Holinsworth,¹ K. R. O'Neal,¹ T. V. Brinzari,¹ D. Mazumdar,¹ Y. Q. Wang,²
S. McGill,³ R. J. Cava,⁴ B. Lorenz,² and J. L. Musfeldt^{1,*}¹*Department of Chemistry, University of Tennessee, Knoxville, Tennessee 37996, USA*²*Department of Physics and TCSUH, University of Houston, Houston, Texas 77204, USA*³*National High Magnetic Field Laboratory, Tallahassee, Florida 32310, USA*⁴*Department of Chemistry, Princeton University, Princeton, New Jersey 08544, USA*

(Received 4 August 2013; revised manuscript received 23 March 2014; published 17 April 2014)

We employ a magnetic-field driven antiferromagnetic to the fully polarized state transition in $\text{Ni}_3\text{V}_2\text{O}_8$ to investigate the interaction between spin ordering and driven charge excitations, with special emphasis on the color properties. Our measurements reveal field-induced blue shifts of the band gap that are much larger than that of the Zeeman effect in isolation, anticipating a more greenish appearance in the fully polarized state. This color change is verified with direct photographic images and emanates from charge density differences around the Ni and O centers in high fields.

DOI: [10.1103/PhysRevB.89.165120](https://doi.org/10.1103/PhysRevB.89.165120)

PACS number(s): 78.20.Bh, 75.30.Kz, 78.20.Ls

I. INTRODUCTION

The band gap is one of the most important electronic energy scales in a solid. It determines a variety of physical properties including *dc* resistivity, and it is vital to a number of applications like light harvesting [1–4]. In both traditional semiconductors and complex oxides, the gap can be manipulated by chemical substitution [2,5], temperature [3,6], pressure [7,8], and electric field [9]. The magnetic field also drives changes in the electronic properties. This effect can be as simple as the textbook case of Zeeman splitting of an isolated atom [10] or as unexpected as amplified spin-charge interactions due to a collective phase transition in a solid [11]. While field-induced band gap changes in conventional semiconductors are of the order of 0.1–0.3 meV/T [12,13], there are only a few examples of large shifts (of the order of 1–10 meV/T) [14]. The discovery of large magnetic-field-induced changes in the optical properties requires reaching beyond traditional mechanisms like the Zeeman effect to include interactions that modify polarizability. Magnetic quantum critical transitions and their associated end points are rich places to search for amplified spin-charge interactions [15]. Moreover, frustrated transition metal oxides are unrivaled in their ability to support competing interactions [16]. Multiferroic $\text{Ni}_3\text{V}_2\text{O}_8$, with small exchange interactions, a frustration index >5 due to the Kagomé staircase structure, and a rich phase diagram with both plateaus and critical fields [17–26], is an attractive system with which to search for strong magnetoelectric-coupling-induced effects.

In this paper, we report the discovery of a visible color change through the antiferromagnetic to fully polarized state transition in $\text{Ni}_3\text{V}_2\text{O}_8$. The 2.35 eV band gap blue shifts by 50 meV between 0 and the 37 T critical field ($B \parallel b$) and saturates in the fully polarized state. This band gap shift makes $\text{Ni}_3\text{V}_2\text{O}_8$ more green (24% at 45 T) [27]. We verify this picture with direct photographic images and discuss the transition in terms of coupling-induced modifications to the charge density. These findings

reveal that key electronic energy scales like the charge gap can be tuned to a surprising extent with external stimuli and that, when major charge excitations appear in the visible range, field-induced shifts can modify the color properties. What makes the field so effective in this case is the presence of a collective transition in combination with strong dynamic magnetoelectric coupling. Other frustrated materials like the rare earth manganites may also display energy transfer processes that mix magnetic quantum fluctuations and dielectric properties.

II. METHODS

$\text{Ni}_3\text{V}_2\text{O}_8$ single crystals were grown from a $\text{BaO-V}_2\text{O}_5$ flux as described previously [18,20], cut to expose the *ac*, *ab*, and *bc* planes, and polished to $\simeq 50 \mu\text{m}$. Variable-temperature spectra were collected using a Bruker Equinox 55 Fourier transform infrared spectrometer equipped with a microscope attachment. Magneto-optical measurements were carried out at the National High Magnetic Field Laboratory using a McPherson 2061A monochromator (0.8–4.1 eV) and both a 35 T resistive magnet and the 45 T hybrid. Absorption was calculated as $\alpha(E) = \frac{-1}{d} \ln(T(E))$, where $T(E)$ is the measured transmittance as a function of energy E , and d is the sample thickness. The latter limits the energy range of our experiments. For the sum rule analysis, we estimated the real part of the refractive index from a Glover-Tinkham analysis [28]. First-principles electronic structure calculations were performed using the Perdew-Burke-Ernzerhof form of the spin-polarized generalized gradient approximation (σ -GGA) [29] and the rotationally invariant scheme of σ -GGA + U [30]. All atomic positions were relaxed within the experimental lattice parameters [19]. The Hubbard U was determined using linear response theory [30,31]. Our calculations focus on two limiting case spin states: the commensurate antiferromagnetic state [18,19] and the ferromagnetic state. We use the latter to approximate the field-induced fully polarized state.

III. RESULTS AND DISCUSSION

Figure 1(a) displays the optical response of $\text{Ni}_3\text{V}_2\text{O}_8$. We assign the broad $\simeq 1.54$ and 1.68 eV bands to ${}^3A_{2g} \rightarrow {}^1E_g$ and

*musfeldt@utk.edu

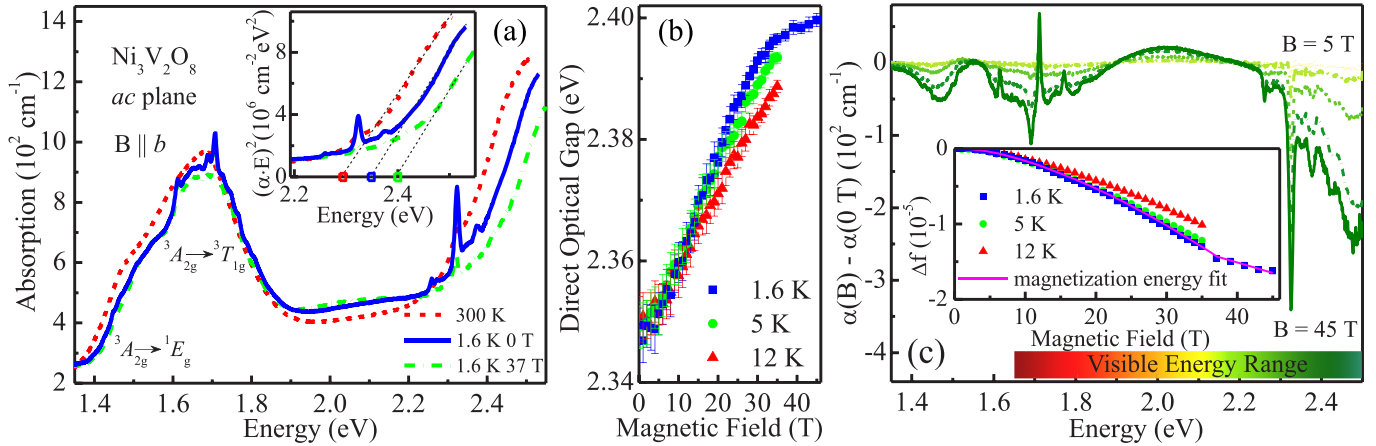


FIG. 1. (Color online) (a) Absorption coefficient, $\alpha(E)$, of $\text{Ni}_3\text{V}_2\text{O}_8$ in the visible range at selected fields and temperatures. Inset: Direct optical gap analysis. The leftmost (red) square marks the 2.29 eV optical gap of $\text{Ni}_3\text{V}_2\text{O}_8$ at 300 K, the center (blue) square marks the 2.35 eV gap at 1.6 K, and the rightmost (green) square marks the 2.40 eV gap at 1.6 K with an applied field of 37 T. (b) Optical gap vs magnetic field at selected temperatures of 1.6, 5, and 12 K. (c) Absorption difference spectra [$\alpha(B) - \alpha(B = 0 \text{ T})$] of $\text{Ni}_3\text{V}_2\text{O}_8$ at 1.6 K for the $B \parallel b$ axis at selected magnetic fields: 5, 10, 20, 35, and 45 T. Inset: Oscillator strength change [$\Delta f = f(B) - f(B = 0 \text{ T})$], which is proportional to the integrated absorption coefficient) in the range of optical gap edge (2.17–2.50 eV) as a function of magnetic field at selected temperatures: 1.6, 5, and 12 K. The magnetization energy [$\alpha \int M(B) dB$, where $M(B)$ is the experimental magnetization and α is a negative constant that depends on whether the system is below or above the critical field; magenta line] [23] fits well with the Δf trend.

${}^3A_{2g} \rightarrow {}^3T_{1g}$ d to d excitations on the Ni^{2+} centers [32]. Another set of on-site excitations (${}^3A_{2g} \rightarrow {}^3T_{2g}$) resides at a lower energy (≈ 0.9 eV) and is not shown [33]. These d - d excitations are formally forbidden but become allowed due to hybridization, exchange interaction, and odd-parity phonons that mix states and break inversion symmetry [11,34,35]. In addition to hybridization with oxygen $2p$ states, there may also be some mixing with unoccupied V states [25]. Resonant inelastic x-ray scattering and crystal field multiplet theory reveal that the crystal field around the cross-tie and spine sites is similar [25]. Charge transfer excitations appear above 2.2 eV in the absorption spectrum and can be assigned as O $2p$ to Ni and V $3d$ hybridized excitations [33,36]. These excitations define the charge gap in $\text{Ni}_3\text{V}_2\text{O}_8$. We find that the gap is 2.35 eV at 1.6 K [37], higher than previously supposed [36,38] but in good agreement with recent x-ray absorption and emission data [25], local density approximation + U calculations for $U = 5$ eV [36], and the shifted partial density of states in Ref. [25]. A linear fit of $(\alpha \cdot E)^2$ vs E [Fig. 1(a), inset] [39] shows that the 2.35 eV band gap is direct. A similarly large optical gap is found in sputtered thin films [40]. Importantly, the ${}^3A_{2g} \rightarrow {}^3T_{1g}$ d -to- d excitation and the band gap are in the visible range and responsible for the dark yellow appearance of $\text{Ni}_3\text{V}_2\text{O}_8$ at 1.6 K. Moreover, the charge gap red shifts by 60 meV between 1.6 and 300 K, similar to that in other oxides [6]. The fine structure riding on top of the on-site excitations and gap edge is assigned as a series of excitons [34]. They soften with increasing temperature.

Magnetic field drives $\text{Ni}_3\text{V}_2\text{O}_8$ from the commensurate antiferromagnetic state at 1.6 K and zero field, through a series of noncollinear regimes, and into the fully polarized paramagnetic state at 37 T for $B \parallel b$ [23]. At the same time, the charge gap moves from 2.35 to 2.40 eV at 1.6 K and 37 T, a blue shift of 50 meV. Between 37 and 45 T, changes in the gap edge are small and within 5 meV, indicating that the optical response

is saturating. Strikingly, the field-induced modification of the gap edge below the critical field (≈ 1.4 meV/T) is greater than the temperature-induced shift (≈ 0.2 meV/K = 0.3 meV/T), and it exceeds what might be expected from the Zeeman effect (4.8 meV at 37 T, 0.13 meV/T) [23] by a considerable amount. This implies that the field is a more effective tuning parameter than the temperature. It also suggests that the excess (beyond that from normal Zeeman interactions) is due to an additional coupling mechanism, as discussed below. Considering the complexity of the B - T phase diagram [18,23], one might anticipate anomalies in the charge gap at the magnetically driven phase transitions. Our data instead reveal that the gap changes smoothly and continuously both below and above the 37 T critical field (Fig. 1(b) and Ref. [33]), with only a slope change as the system goes into the fully polarized state. The field-induced blue shift is slightly less at higher temperatures due to thermal broadening effects. Turning briefly to the other spectral features, the intensity of the d - d excitations decrease with field, behavior also observed in hematite [11], although the spin-flop transition in α - Fe_2O_3 is much less effective at amplifying magnetoelectric coupling than the antiferromagnetic to fully polarized state transition in $\text{Ni}_3\text{V}_2\text{O}_8$. We also find that the exciton peak positions track the magnetization energy [33]. In the following discussion, we focus on the gap behavior and its relation to color property modifications.

Figure 1(c) displays the magnetic-field-induced absorption difference spectra of $\text{Ni}_3\text{V}_2\text{O}_8$. In high field, this system absorbs fewer photons in the green color range (on the order of 24% less at 45 T) [27]. $\text{Ni}_3\text{V}_2\text{O}_8$ thus appears more green in the fully polarized paramagnetic state than at zero field. We quantify the field-induced color change with the partial sum rule [Fig 1(c), inset]: $f \equiv \frac{2c}{N_e \hbar \pi \omega_p^2} \int_{E_1}^{E_2} n \alpha(E, B) dE$ [39]. Here, $N_e = 2$ is the number of electrons per Ni site, $n \approx 2.13$ is the refractive index, ω_p is the plasma frequency, $\equiv \sqrt{\frac{e^2 \rho}{m \epsilon_0}}$, e and

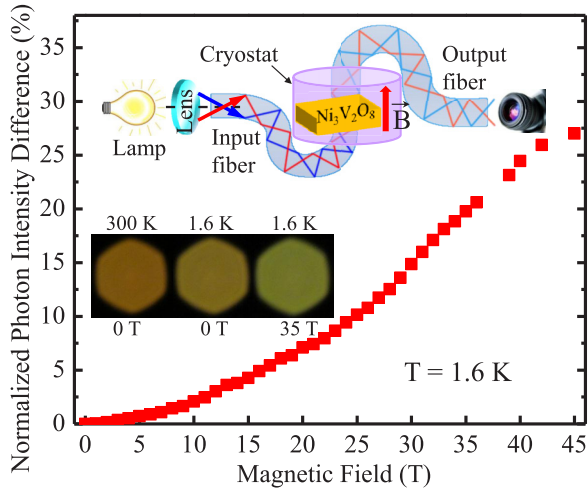


FIG. 2. (Color online) Photon intensity difference as a function of magnetic field in the green color range (2.17–2.50 eV). This represents the green color change shown in the photos. Top inset: Schematic of the experimental setup. We took pictures through the optical fibers (1 mm diameter, 370–2000 nm; Canon Powershot SX30 IS) with a xenon source. Bottom inset: Photos of $\text{Ni}_3\text{V}_2\text{O}_8$ single crystals under different temperature and field conditions for $B \parallel b$.

m are the charge and mass of an electron, ϵ_0 is the vacuum dielectric constant, $\rho = 2.17 \times 10^{28} \text{ m}^{-3}$ is the density of Ni sites, c is the speed of light, and $E_1 = 2.17 \text{ eV}$ and $E_2 = 2.50 \text{ eV}$ are the energy limits of integration. We find that oscillator strength decreases with applied field and that the overall trend is well described by the magnetization energy $\alpha \int M(B) dB$, where $M(B)$ is the experimental magnetization and α is a (negative) constant that depends on proximity to the 37 T critical field [Fig 1(c), inset] [23]. α is large below the critical field due to a combination of magnetoelectric coupling and Zeeman interactions [41]. Coupling is diminished in the fully polarized state, where the field-induced change in oscillator strength (Δf) is described solely by the Zeeman effect [42].

Motivated by these spectroscopic findings, we sought direct visual confirmation of the field-induced color change in $\text{Ni}_3\text{V}_2\text{O}_8$. This evidence was obtained by replacing the spectrometer with a black box and taking pictures of the light brought in by optical fiber under various magnetic fields. The setup and photographic outcomes are summarized in Fig. 2. Clearly, the color of $\text{Ni}_3\text{V}_2\text{O}_8$ changes with temperature and magnetic field. Upon warming from 1.6 to 300 K, the reddish-yellow aspect of the crystal is enhanced while the green tones are diminished. This is a simple temperature broadening effect. By contrast, application of a magnetic field at low temperatures enhances the greenish appearance. As discussed below, this is a consequence of combined magnetoelectric coupling and Zeeman interactions. The color differences captured with our black box + camera setup are consistent with the magneto-optical data in Fig. 1. To quantify how much green color is gained, we calculated the photon intensity in the 2.17 to 2.50 eV green spectral range and show the variation $[\frac{\int I(E,B)dE - \int I(E,0T)dE}{\int I(E,0T)dE}]$ as a function of the applied field (Fig. 2). Here, $I(E, B)$ is the photon intensity at

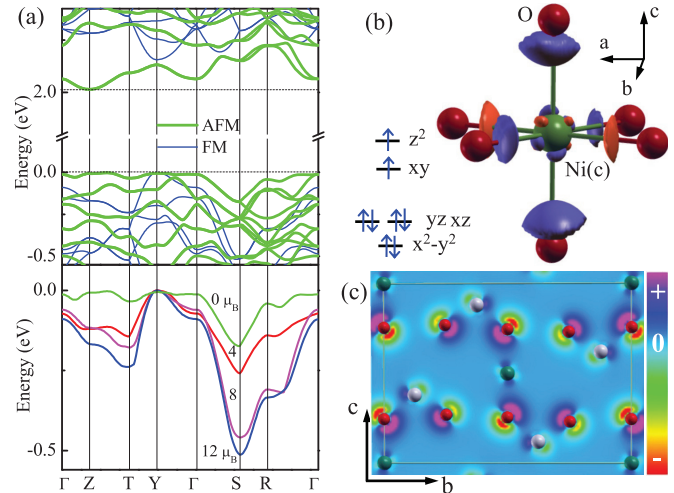


FIG. 3. (Color online) (a) Top: Band structure of $\text{Ni}_3\text{V}_2\text{O}_8$ with antiferromagnetic and ferromagnetic ordering in the region of the band gap. Calculated direct gaps are 2.02 and 2.15 eV in the antiferromagnetic and ferromagnetic state, respectively. In the ferromagnetic state, only the majority band structure is shown for clarity. The valence- and conduction-band edges in the antiferromagnetic state are indicated by dashed horizontal lines. Computed Hubbard U 's are 4.0 and 4.2 eV for Ni(c) and Ni(s) ions, respectively [30]. Bottom: Valence band structure with the total spin moment fixed at 0, 4, 8, and $12 \mu_B$. (b) Charge density difference $[\Delta\rho = \rho(\text{FM}) - \rho(\text{AFM})]$ around the Ni cross-tie center. The isosurface is $\pm 0.014 e/\text{\AA}^3$. The positive (negative) value is represented in blue (red). The smaller diagram at the lower left illustrates the electron configuration of a $d^8 \text{ Ni}^{2+}$ center. (c) $\Delta\rho$ projected onto the bc plane. The charge density scale is from -0.08 to $0.04 e/\text{\AA}^3$.

energy E and magnetic field B . We find that the green intensity increases by 20% at 35 T and 27% at 45 T—a huge effect.

To understand the field-induced color change mechanism, we calculate the electronic structure in two different limiting-case spin states and extracted charge density (ρ) differences [43,44]. The band structure reveals a direct gap character in both the antiferromagnetic and ferromagnetic phases, although the gap shifts from the Z to Y point and is predicted to increase slightly in the ferromagnetic state [Fig. 3(a), top]. These findings are in agreement with our magneto-optical spectra. To investigate how the band structure evolves between the antiferromagnetic and the ferromagnetic states, we gradually increased spin polarization away from the fully compensated situation [Fig. 3(a), bottom]. Away from the Y point, the valence band energy systematically decreases with increasing moment. As the fundamental gap excitation shifts from Z in the antiferromagnetic state to Y in the ferromagnetic state, the gap increases. We therefore expect that the optical properties will be different at 0 T and full field, in agreement with our experimental findings.

The charge density difference between the two limiting-case spin states captures the mixing between charge and magnetism in $\text{Ni}_3\text{V}_2\text{O}_8$. Figure 3(b) displays total charge density difference contours around the Ni cross-tie center. This plot reveals that the charge density of the d_{xy} and $d_{3z^2-r^2}$ states increases in the ferromagnetic state, whereas that of the d_{xz} and d_{yz} states is reduced. The O $2p$ density due to Ni-O bonding

near the Ni(c) site is simultaneously enhanced. The charge around the Ni(s) center is also distorted. Figure 3(c) shows a projection of the charge density difference onto the bc plane. In the ferromagnetic state, the O $2p$ state density changes by approximately $\pm 3\%$, ρ of the Ni $3d$ states is modified by about $\pm 1.5\%$, and ρ of the V $3d$ states changes less than $\pm 1\%$ [45]. These findings demonstrate that charge density (especially that around the O center) is redistributed through the collective transition. This redistribution modifies the charge excitations in $\text{Ni}_3\text{V}_2\text{O}_8$. Changes in local charge density also drive magnetoelectric effects in molecular systems [46].

Bringing these results together, we propose that the field-induced blue shift of the optical band gap in $\text{Ni}_3\text{V}_2\text{O}_8$ can be understood in terms of magnetoelectric coupling. Zeeman interactions certainly move the system toward the fully polarized state in applied field. But what really accelerates the process is the spin-charge coupling in which the high field spin state redistributes charge density around the Ni and O sites, differentiating it from that under zero-field conditions. Polarizability at the Ni and O centers provides this flexibility. Since nearest-neighbor magnetic coupling arises from superexchange interactions mediated by Ni-O-Ni linkages, the O $2p$ charge density also becomes asymmetric, increasing near the Ni sites and decreasing on the opposite side. These field-induced charge density distortions modify the electronic structure and shift the band gap toward higher energy. Once the system is in the fully polarized state, the spin moment is saturated and this mechanism no longer contributes.

Since $\text{Ni}_3\text{V}_2\text{O}_8$ is an insulator, we can use the ratio of the gap difference to the magnetization energy in the fully polarized state to estimate the magnitude of spin-charge coupling. Using the 50 meV blue shift of the gap through the 37 T critical field and a magnetization energy of 4.8 meV [23], we find a dynamic coupling constant of ≈ 10 , which is very large. By contrast, the static polarization induced by the magnetic field has a maximum value of $60 \mu\text{C}/\text{m}^2$ and goes to 0 above 12 T

[23]. Thus, we see that the same mechanism gives different results at ac and dc frequencies [17,23]. The former refers to the ability of the applied magnetic field to modify driven excitations, whereas the latter refers to the ability of a magnetic field to manipulate charge in the static limit. The magnetoelectric coupling mechanism is the same in these two cases.

IV. SUMMARY

Summarizing, we report the discovery of dynamic magnetoelectric coupling in $\text{Ni}_3\text{V}_2\text{O}_8$ through the antiferromagnetic to fully polarized state transition and the manifestation of this coupling as a magnetic field-induced blue shift of the 2.35 eV optical gap. The shift of this key electronic energy scale is large (1.4 meV/T below the 37 T critical field)—substantially more than the Zeeman contribution in isolation (0.13 meV/T). The difference arises from the ability of the collective transition to amplify spin-charge interactions. We verify these spectroscopic findings with direct photographic images of $\text{Ni}_3\text{V}_2\text{O}_8$ and analyze the color contrast in terms of differences in the local charge density around the Ni and O centers. Similar energy transfer processes and mechanisms may mix magnetic quantum fluctuations and the dielectric response in other materials [47,48].

ACKNOWLEDGMENTS

We thank M. Cococcioni, S. de Gironcoli, G. Lawes, M. R. Pederson, and J. F. Wang for useful discussions. This research was supported by the Materials Science Division, Basic Energy Sciences, U.S. Department of Energy [Contract No. DE-FG02-01ER45885 at UT (J.L.M.), No. DE-AC03-76SF00098 at TCSUH (B.L.), and No. DE-FG02-45706 at Princeton (R.J.C.)]. Work at the NHMFL was supported by the National Science Foundation (Grant No. DMR-0084173).

-
- [1] S. J. Pearton, C. R. Abernathy, M. E. Overberg, G. T. Thaler, D. P. Norton, N. Theodoropoulou, A. F. Hebard, Y. D. Park, F. Ren, J. Kim, and L. A. Boatner, *J. Appl. Phys.* **93**, 1 (2003).
 - [2] Ü. Özgür, Ya. I. Alivov, C. Liu, A. Teke, M. A. Reshchikov, S. Doğan, V. Avrutin, S.-J. Cho, and H. Morkoç, *J. Appl. Phys.* **98**, 041301 (2005).
 - [3] S. R. Basu, L. W. Martin, Y. H. Chu, M. Gajek, R. Ramesh, R. C. Rai, X. Xu, and J. L. Musfeldt, *Appl. Phys. Lett.* **92**, 091905 (2008).
 - [4] T. Choi, S. Lee, Y. J. Choi, V. Kiryukhin, and S.-W. Cheong, *Science* **324**, 63 (2009).
 - [5] V. Yu. Davydov, A. A. Klochikhin, V. V. Emtsev, S. V. Ivanov, V. V. Vekshin, F. Bechstedt, J. Furthmüller, H. Harima, A. V. Mudryi, A. Hashimoto, A. Yamamoto, J. Aderhold, J. Graul, and E. E. Haller, *Phys. Status Solidi B* **230**, R4 (2002).
 - [6] D. Qian, L. Wray, D. Hsieh, D. Wu, J. L. Luo, N. L. Wang, A. Kuprin, A. Fedorov, R. J. Cava, L. Viciu, and M. Z. Hasan, *Phys. Rev. Lett.* **96**, 046407 (2006).
 - [7] J. Ruiz-Fuertes, S. López-Moreno, J. López-Solano, D. Errandonea, A. Segura, R. Lacomba-Perales, A. Muñoz, S. Radescu, P. Rodríguez-Hernandez, M. Gospodinov, L. L. Nagornaya, and C. Y. Tu, *Phys. Rev. B* **86**, 125202 (2012).
 - [8] A. G. Gavriliuk, V. V. Struzhkin, I. S. Lyubutin, S. G. Ovchinnikov, M. Y. Hu, and P. Chow, *Phys. Rev. B* **77**, 155112 (2008).
 - [9] K. F. Mak, C. H. Lui, J. Shan, and T. F. Heinz, *Phys. Rev. Lett.* **102**, 256405 (2009).
 - [10] N. W. Ashcroft, and N. D. Mermin, *Solid State Physics* (Brooks Cole, Pacific Grove, CA, 1976).
 - [11] P. Chen, N. Lee, S. McGill, S.-W. Cheong, and J. L. Musfeldt, *Phys. Rev. B* **85**, 174413 (2012).
 - [12] K. Uchida, N. Miura, J. Kitamura, and H. Kukimoto, *Phys. Rev. B* **53**, 4809 (1996).
 - [13] P. Bhattacharya, R. Fornari, and H. Kamimura, *Comprehensive Semiconductor Science and Technology*, Vol. 2 (Elsevier Science, New York, 2011).

- [14] G. Fedorov, P. Barbara, D. Smirnov, D. Jiménez, and S. Roche, *Appl. Phys. Lett.* **96**, 132101 (2010).
- [15] S. Sachdev, *Quantum Phase Transitions*, 2nd ed. (Cambridge University Press, Cambridge, UK, 2011).
- [16] A. P. Ramirez, *Annu. Rev. Mater. Sci.* **24**, 453 (1994).
- [17] P. Kharel, C. Sudakar, A. Dixit, A. B. Harris, R. Naik, and G. Lawes, *Europhys. Lett.* **86**, 17007 (2009).
- [18] G. Lawes, M. Kenzelmann, N. Rogado, K. H. Kim, G. A. Jorge, R. J. Cava, A. Aharony, O. Entin-Wohlman, A. B. Harris, T. Yildirim, Q. Z. Huang, S. Park, C. Broholm, and A. P. Ramirez, *Phys. Rev. Lett.* **93**, 247201 (2004).
- [19] M. Kenzelmann, A. B. Harris, A. Aharony, O. Entin-Wohlman, T. Yildirim, Q. Huang, S. Park, G. Lawes, C. Broholm, N. Rogado, R. J. Cava, K. H. Kim, G. Jorge, and A. P. Ramirez, *Phys. Rev. B* **74**, 014429 (2006).
- [20] R. P. Chaudhury, F. Yen, C. R. de la Cruz, B. Lorenz, Y. Q. Wang, Y. Y. Sun, and C. W. Chu, *Phys. Rev. B* **75**, 012407 (2007).
- [21] T. Lancaster, S. J. Blundell, P. J. Baker, D. Prabhakaran, W. Hayes, and F. L. Pratt, *Phys. Rev. B* **75**, 064427 (2007).
- [22] I. Cabrera, M. Kenzelmann, G. Lawes, Y. Chen, W. C. Chen, R. Erwin, T. R. Gentile, J. B. Leão, J. W. Lynn, N. Rogado, R. J. Cava, and C. Broholm, *Phys. Rev. Lett.* **103**, 087201 (2009).
- [23] J. F. Wang, M. Tokunaga, Z. Z. He, J. I. Yamaura, A. Matsuo, and K. Kindo, *Phys. Rev. B* **84**, 220407(R) (2011).
- [24] The critical fields for saturation of the magnetization are 35, 37, and >48 T for fields along the a , b , and c axis, respectively [23].
- [25] J. Laverock, B. Chen, A. R. H. Preston, K. E. Smith, N. R. Wilson, G. Balakrishnan, P.-A. Glans, and J.-H. Guo, *Phys. Rev. B* **87**, 125133 (2013).
- [26] G. Ehlers, A. A. Podlesnyak, S. E. Hahn, R. S. Fishman, O. Zaharko, M. Frontzek, M. Kenzelmann, A. V. Pushkarev, S. V. Shiryayev, and S. Barilo, *Phys. Rev. B* **87**, 214418 (2013).
- [27] The green spectral range is 2.17–2.50 eV.
- [28] M. Tinkham, in *Far Infrared Properties of Solids*, edited by S. S. Mitra and S. Nudelman (Plenum, New York, 1970), p. 233.
- [29] J. P. Perdew, K. Burke, and M. Ernzerhof, *Phys. Rev. Lett.* **77**, 3865 (1996).
- [30] M. Cococcioni and S. de Gironcoli, *Phys. Rev. B* **71**, 035105 (2005).
- [31] T. Tsuchiya, R. M. Wentzcovitch, C. R. S. da Silva, and S. de Gironcoli, *Phys. Rev. Lett.* **96**, 198501 (2006).
- [32] W. Low, *Phys. Rev.* **109**, 247 (1958).
- [33] See Supplemental Material at <http://link.aps.org/supplemental/10.1103/PhysRevB.89.165120> for details on the other set of on-site excitations.
- [34] D. D. Sell, R. L. Greene, and R. M. White, *Phys. Rev.* **158**, 489 (1967).
- [35] Ni(c) has C_{2h} site symmetry, whereas distortion breaks the inversion center on Ni(s), reducing it to C_2 [33]. This symmetry breaking activates the formally Laporte forbidden excitations. The weak ${}^3A_{2g} \rightarrow {}^1E_g$ shoulder is also spin forbidden but becomes allowed due to spin-orbit and exchange interactions that hybridize states.
- [36] R. C. Rai, J. Cao, S. Brown, J. L. Musfeldt, D. Kasinathan, D. J. Singh, G. Lawes, N. Rogado, R. J. Cava, and X. Wei, *Phys. Rev. B* **74**, 235101 (2006).
- [37] We determined the optical gap using the leading edge of the charge transfer excitation, therefore, the absolute gap value may be somewhat underestimated. The field-induced effect will not be impacted by gap determination.
- [38] An insufficient integration range in the Kramers-Kronig analysis may be responsible for the previously underestimated optical band gap [36].
- [39] F. Wooten, *Optical Properties of Solids* (Academic Press, New York, 1972).
- [40] A. Dixit, P. Chen, J. L. Musfeldt, and G. Lawes (unpublished).
- [41] The fit shows that the magnetoelectric coupling is also proportional to the magnetization energy.
- [42] The response broadens with temperature over the full field range as expected.
- [43] The Hubbard U plays its role by enlarging the band gap.
- [44] Here we use the ferromagnetic spin arrangement to model that in the fully polarized state.
- [45] The charge density difference around Ni(s) does not show a precise, characteristic d orbital shape due to a slight octahedral distortion.
- [46] Ö. Günaydin-Şen, P. Chen, J. Fosso-Tande, T. L. Allen, J. Cherian, T. Tokumoto, P. M. Lahti, S. McGill, R. J. Harrison, and J. L. Musfeldt, *J. Chem. Phys.* **138**, 204716 (2013).
- [47] M. Jaime, R. Daou, S. A. Crooker, F. Weickert, A. Uchida, A. E. Feiguin, C. D. Batista, H. A. Dabkowska, and B. D. Gaulin, *Proc. Natl. Acad. Sci. USA* **109**, 12404 (2012).
- [48] P. Jiang, J. Li, A. W. Sleight, and M. A. Subramanian, *Inorg. Chem.* **50**, 5858 (2011).